

Investigation of the Impact of Future Emission Norms on the Axial Force System in Turbochargers using Measurements and Numerical Methods

Richárd Takács*

Széchenyi István University, Department of Internal Combustion Engines and Drivetrains, Egyetem tér 1, 9026, Győr Hungary

***Corresponding Author:** Richárd Takács, Széchenyi István University, Department of Internal Combustion Engines and Drivetrains, Egyetem tér 1, 9026, Győr Hungary.

Received: March 09, 2023; **Published:** March 24, 2023

Abstract

The use of turbochargers nowadays is growing rapidly. However, compliance with stricter environmental regulations for internal combustion engines and the need to reduce fuel consumption are emerging in the above-mentioned group of components. The documentation describes the analytical determination, measurement options and the impact on the turbocharger of axial loads, also known as axial loads, in various publications. The resulting axial force, due to the narrow axial tolerance ranges used in the turbocharger, can cause damage to its structure above a certain level. To avoid this, a so-called axial bearing is installed which, together with the damping effect of the surrounding oil film, prevents excessive rotation of the rotating part in the axial direction. However, under certain conditions, the presence of the oil film between the rotating unit and the stationary axial bearing may be eliminated by heavy stress, so that not only significant friction, but also damage to the bearings and ultimately, the turbocharger may occur. In order to avoid injuries and reduce the friction losses of the charger, it is necessary to define the stresses present here as accurately as possible and to simulate the effect of changing conditions. The purpose of this document is to process the methods and knowledge of this publication in various publications, and to assess further research options that model the impact of the stress caused by EURO 7 and further environmental standards.

Keywords: turbocharger; axial force; emission; internal combustion engines

Introduction

The aim of the documentation is to create a complex picture of the factors, calculation possibilities and the impact on the system of the progress of the axial force in turbochargers by processing the knowledge of various published publications and literature. During the study, we can learn about the importance of using an axial bearing closely related to this force, the criteria for its design, and the effects of its damage. Another aim is to research further develop methods and test options based on the experience gained during document processing, which models the impact of the gradual tightening of environmental standards and other demands on the system.

The axial bearing of the turbocharger

The pulse of the gas streams on both the turbine and the compressor side, as well as the different pressure conditions of the two sides, force the turbocharger rotor unit into axial movement. Therefore, in order to adhere to the narrow range tolerances and to protect the used seals, a so-called axial bearing is typically installed as shown below.



Figure 1: Sectional view of a turbocharger [1].

Both sides of the axial bearing come in contact with a lubricating oil film, which serves as a damping agent between the stationary axial bearing and the axially moving parts. The figure below shows this part with number 2.

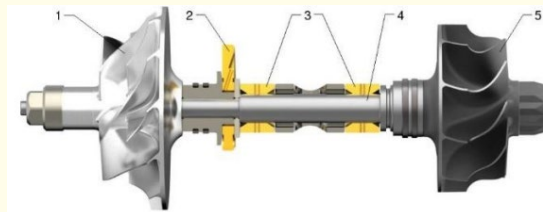


Figure 2: Sectional view of a turbocharger's rotating unit.

The axial bearing has a fixed position in the turbocharger, so is the load of the rotor, but it is also a significant load for the typically high-temperature environment. The basic material used is generally lead-bronze.

Emphasized publications in the topic of axial force of the turbocharger

In this chapter, published publications on the possibilities of detecting axial force in the turbochargers, the causes of its occurrence and the consequences of its presence are presented, aiming to provide further development based on extensive experience.

The [1] publication presents the lubrication system of the axial bearings of turbochargers first. The axial bearing is fixed to the middle part, while the axial ring rotates with the shaft. In order to achieve a friction-free realization of relative displacement, it is necessary to have the right amount and quality of oil / lubricant. The axial displacement caused by the axial load is compensated by the oil / lubricant applied to the two sides of the bearing. The axial force action is due to different pressures and mass flows inside of the turbocharger's compressor and turbine. These parameters depend primarily on the speed of the rotor, which can also show rapid changes due to the dynamic operation of the internal combustion engine. This documentation offers two options for calculating the axial load. The first method offers a highly accurate but time-consuming solution in a simulation environment with CFD method. Changing any parameter means re-generation or run time. Newton's second law that offers less than 10% deviation from the CFD method, based on measurements by writers in the documentation, offers more flexible and faster reporting. The input parameters for the calculation are the followings:

- Pressure before the compressor (p_1).
- Pressure after the compressor (p_2).

- Pressure before the turbine (p_3).
- Pressure after the turbine (p_4).
- Mass flow on the compressor (\dot{m}_c).
- Mass flow on the turbine (\dot{m}_t).

The following figure shows the summary of all these parameters.

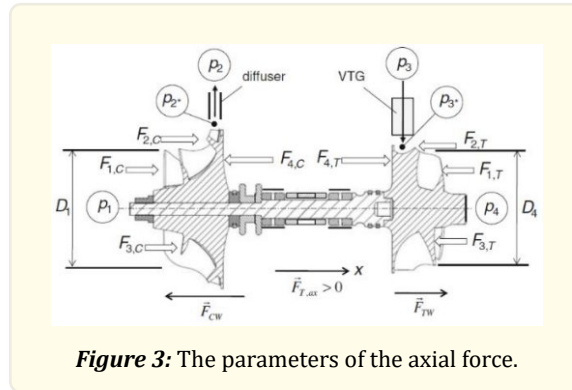


Figure 3: The parameters of the axial force.

The compressor inlet (F_{1C}) pressure can be determined as follows:

$$F_{1C} = A_1 p_1 = \frac{\pi D_1^2}{4} p_1 \quad (1)$$

Where:

- D_1 : compressor inlet diameter.
- p_1 : pressure before the compressor.

The F_{2C} pressure can be calculated using the following formula:

$$F_{2C} = A_s \left(\frac{p_1 + p_2^*}{2} \right) \quad (2)$$

Where:

- p_2^* : pressure value of the compressed air at the compressor's trailing edge
- A_s : is the projected area of the shroud surface.

After determining the pressure values, it is necessary to calculate the force resulting from the mass flow and velocity of the air:

$$F_{3C} = \frac{\dot{m}_c^2 R_a T_1}{p_1 A_{in}} \quad (3)$$

Where:

- \dot{m}_c : air mass flow on the compressor.
- R_a : gas constant of the air.
- T_1 : temperature of the inlet air.
- p_1 : pressure of the inlet air.
- A_{in} : inlet cross-section of the compressor.

The force on the back of the compressor can be determined from the pressure value present and the size of the active surface:

$$F_{4C} = A_{bf} p_2^* \quad (4)$$

Where:

- A_{bf} : the active surface of the compressor's back face.

The turbine side parameters can be calculated just like the ones listed above. This allows us to determine the actual axial force.

$$F_{Tax} = F_{CW} + F_{TW} \quad (5)$$

In order to determine the p_2^* and the p_3^* values, the authors of this book find a solution by means of an authoritative analysis, which come from the rate of the enthalpy growth in the compressor and the enthalpy growth during the compression, as well as the enthalpy reduction in the turbine and enthalpy growth during the expansion. In the case of a compressor, this measure (r_c) can be 55-60% taking into account all operating points.

$$p_2^* = p_1 \left[1 + r_c \left(\left(\frac{p_2}{p_1} \right)^{\frac{\kappa_a - 1}{\kappa_a}} - 1 \right) \right]^{\frac{\kappa_a}{\kappa_a - 1}} \quad (6)$$

Where κ_a : isentropic exponent of the charge air.

In the case of the turbine, this number (r_t) can be different depending on the applied construction. When using wastegate, it can be around 50% for every working point, and 20-90% for VTG depending on its openness.

$$p_3^* = p_4 \left[1 + r_T \left(\left(\frac{p_3}{p_4} \right)^{\frac{\kappa_g - 1}{\kappa_g}} - 1 \right) \right]^{\frac{-\kappa_g}{\kappa_g - 1}} \quad (7)$$

However, to obtain accurate data, it is suggested to use measurements instead of approximate formulas.

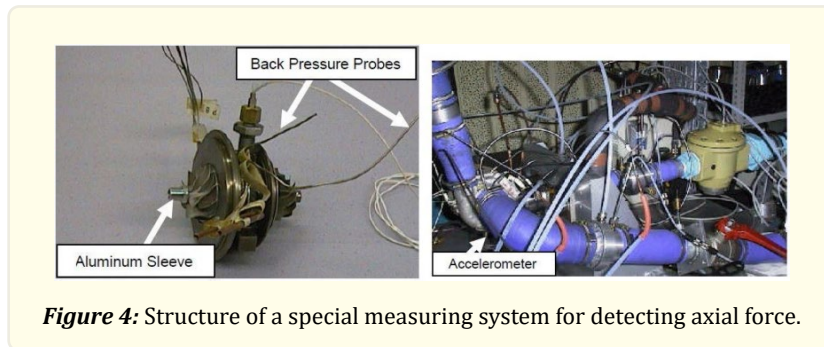
The authors of the [2] publication have developed a special measuring system specifically for measuring axial force. The change in the axial force was simulated by the opening angle of a throttle valve on the inlet and outlet side of the compressor. Static and dynamic characteristics were also measured. They were looking for a connection between the aerodynamic performance of the turbocharger and the resulting axial load. The relationship between the axial load, the lateral movement of the rotating group, and the radial vibration have also been determined (all in the bearing housing of the turbocharger). There was no significant axial force during low-speed ranges, so the rotating group did not suffer any major axial displacement or oil leakage. They wanted to prove the results of the measurements with approximate analytical calculations. They mention the increasing stress on the turbocharger bearings due to the increased temperature load, the need to produce an increasing pressure ratio, and the mechanical load caused by the extremely highspeed ranges, coupled with increasingly low-viscosity lubricants to reduce friction values. It is mentioned that the variable geometry turbine construction can further increase the magnitude of the axial force. It discusses the increase in noise levels resulting from increased stress, which is also a major challenge for development engineers.

Similarly to the previous literature, they are derived from the static pressure values on the compressor and turbine side and from the resulting mass flows. The documentation demonstrates the measurement of the axial force and the determination of its characteristics through a physical experiment of a special test device. The aerodynamic performance of the turbocharger and the correlation between the developed axial force were studied primarily. The interaction between axial load, lateral movement of rotors and radial vibrations of the middle part have also been defined. The analytical calculations associated with the measurements gave a good approximation of the results.

The measurement of the axial force is similar to the previous publication. Linear correlation has been established in calculating the pressure values with increasing the distance from the shaft. The inertial forces are illustrated and explained by reversing the speed directions by 90 °.

The construction shown in Figure 4 was created to perform the measurements. The bearing system, in this case, is semi-floating, so

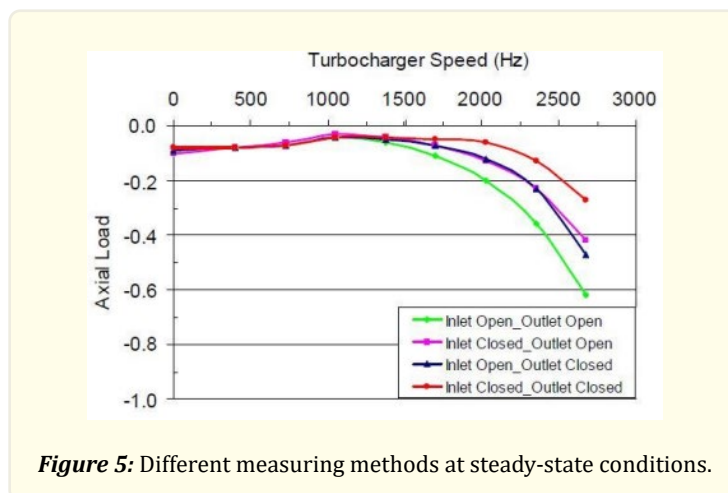
the lubricant is only placed between the shaft and the radial bearing. A non-rotating pin inserted in the middle section with the strain gauge placed on it prevents the axial displacement of the radial bearing and also measures the current axial force. The strain gauges were individually calibrated for the 0-150N force range. The static pressure on the back face of the wheels was measured with inbuilt sensors. An aluminium ring was also mounted on the compressor-side shaft end for mapping the phenomenon of tap motion, and an accelerometer sensor was also installed in the middle part to detect radial vibrations.



The compressor mass flow was measured, and several pressure and temperature sensors were installed to provide the most accurate results possible. With the help of throttle valves built in front of and behind the compressor, four different states, four different axial load levels, were created.

1. Inlet opened-outlet opened.
2. Inlet closed with 45°-outlet opened.
3. Inlet closed with 45°-outlet closed with 45°.
4. Inlet opened-outlet closed with 45°.

After three measurements of each configuration, the authors found good reproducibility. Two types of measurement strategies are also presented. Measurements were made in static work points and during pre-defined dynamic tests. The latter was accelerated with 40 Hz/s between 400Hz and 2700Hz. The lubricating oil used was of 15W40 quality, with an inlet pressure of 4.2 bar and a temperature of 30 °C. Under steady-state conditions, the four measurement methods showed the following results:



The general tendency showed that the axial force evolving in the direction of the predetermined directions is negative, i.e. from the compressor to the turbine. The results showed an excellent approximation in dynamic conditions compared to the interpolated curves of static measurements.

The following diagram shows the axial load measured at static work points together with the compressor map of the compressor.

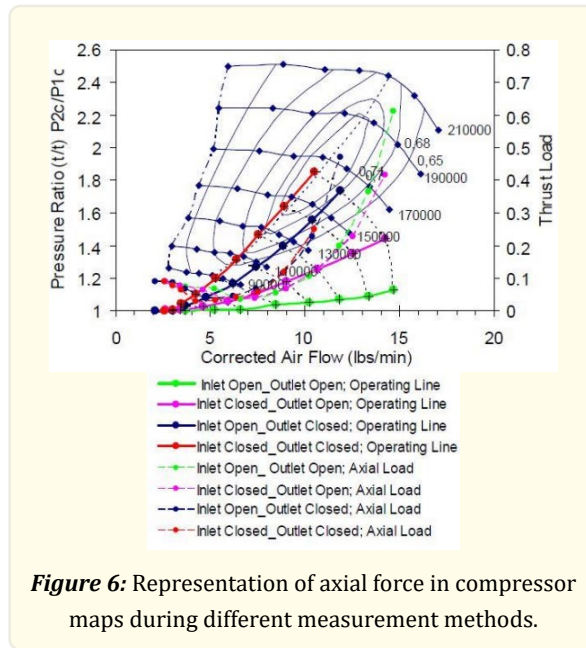


Figure 6: Representation of axial force in compressor maps during different measurement methods.

It can be seen that axial force measurement with valves open before and after the compressor is located in the lower right half of the compressor map, which is not relevant to the actual engine operating range. However, the measurement with the 45° closed inlet and outlet valve is already visible within this range.

Measurements carried out with different configurations gave a good approximation to the analytically calculated values, however, they emphasize that the air mass flow on the compressor and the turbine side was assumed to be equal, which may differ under real conditions. The figure below shows the magnitude of the various force components determining the axial force at a turbo speed of 160,000 rpm.

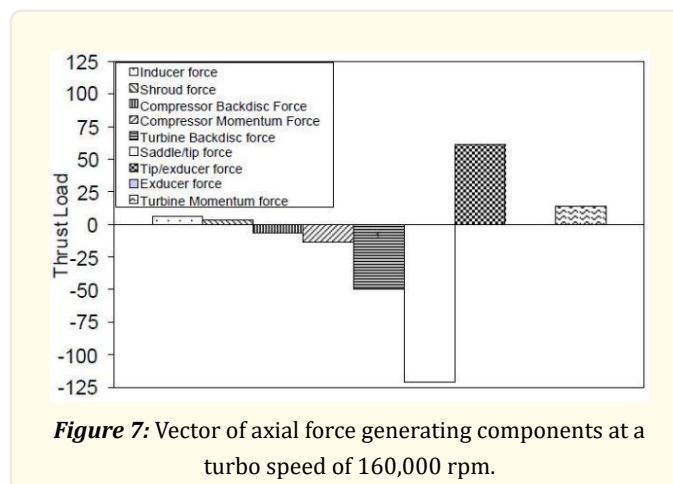


Figure 7: Vector of axial force generating components at a turbo speed of 160,000 rpm.

The [3] publication's authors' work primarily aimed to raise the design method of axial bearings to a higher level. The presence of the axial force is considered to be one of the main actors of the friction in the turbocharger [4, 5], which in the case of excessive values damages the efficiency of the turbocharger [6]. The documentation wants to give a precise description of the method of calculating this kind of force, based on the [7] publication. As a first step, the relationship between the parameters responsible for the emergence of the axial force and the resulting deformation must be determined and then subjected to numerical control. In the next step, the measured deformation signal is corrected on the basis of the temperature load.

They introduce, that damage to the axial bearing in the turbocharger not only results in loss of performance and loss of efficiency, but can also lead to the failure of the entire structure, and therefore it is considered important to define the axial force. It was tested numerically and by measurement, especially near full load, choke limit and pumping limit. With a special test device, a connection has been established between the applied axial force and the resulting stretches. It is important to mention that during the measurements, temperature values were also detected in order to remove the elongation resulting from the thermal expansion from the elongation value due to the actual mechanical load.

The sign of the strain gauge stamps on the compressor side of the axial bearing determines the direction of the axial force that is currently developing, takes the positive sign from the turbine to the compressor.

With the help of a special measuring system, besides causing a defined axial force, they wanted to establish a connection between this force and the appearing elongation. This can be seen in Figure 8.

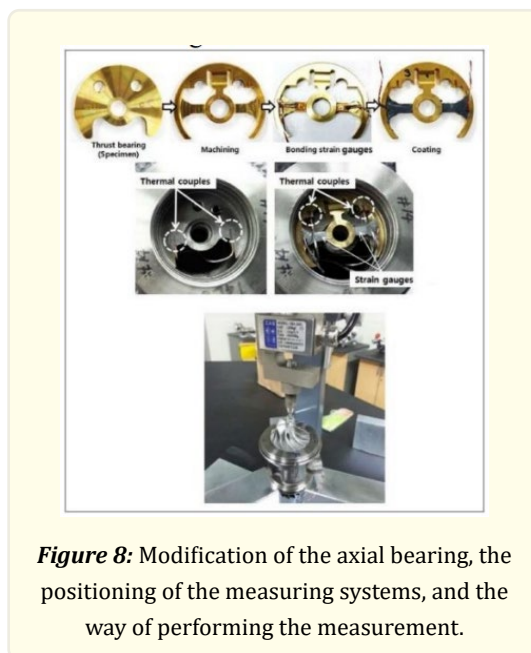


Figure 8: Modification of the axial bearing, the positioning of the measuring systems, and the way of performing the measurement.

For better detection of the measurement results, the original geometry of the axial bearing was modified as shown in the picture above. The force measurement experiments were done in both directions. With 200 N and 250 N load forces, the axial bearing remained in the elastic deformation phase.

Measurements based on finite element methods were also performed, using second order tetrahedral elements, and the grips were applied on bearing contact surfaces according to the direction of the current load force. The results of the finite element simulations show that the highest stress values have fallen to the area where the strain gauges have been placed.

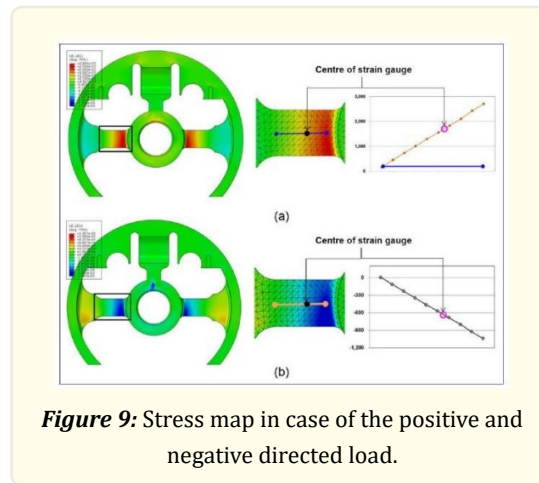


Figure 9: Stress map in case of the positive and negative directed load.

The diagrams on the right side of the image illustrate a horizontal change in the direction of the elongation following axial force. Data from the measurement and finite element test results show a satisfactory approximation. The function of these diagrams provides an excellent description of the relationship between the resulting axial force and the resulting elongation values.

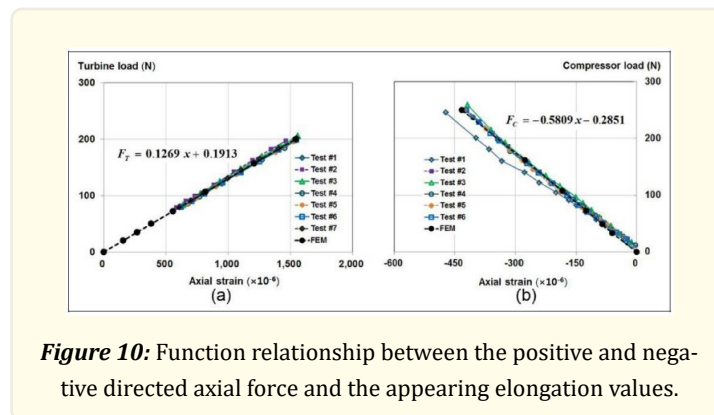


Figure 10: Function relationship between the positive and negative directed axial force and the appearing elongation values.

F_T is the axial force showing in the direction from the turbine to the compressor, and F_C is the axial force showing in the direction from the compressor to the turbine. Using the experience described earlier, the current axial force can be determined inversely from the current elongation and temperature values. In this documentation, a full load test of a 1.4-litre diesel engine was carried out in both the hot gas component test pad and the engine testbench. During the tests, the turbocharger contained the axial bearing in the documentation, and the temperature and elongation values were measured as described above.

On the left-hand side of the following figure, the turbocharger speed detected during this full load test can be seen in relation to the engine speed. On the right side of the image, this can also be seen in the compressor field.

In another figure, the direction and magnitude of the axial force formed can be observed in the compressor field. It can be stated that near the surge line there is a low amplitude force from the turbine to the compressor, while at the limit of choke there is an order of magnitude greater in the opposite direction. Measurements have been made along the curve of the best efficiency points for the different speeds, with a slight negative force. Measurements were made on a hot gas component test bench.

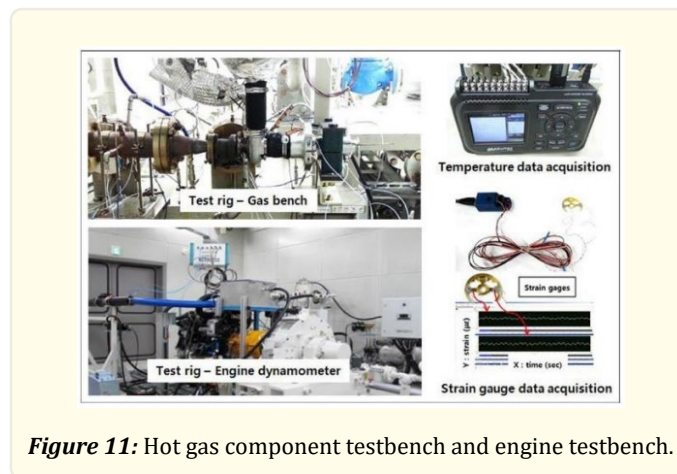


Figure 11: Hot gas component testbench and engine testbench.

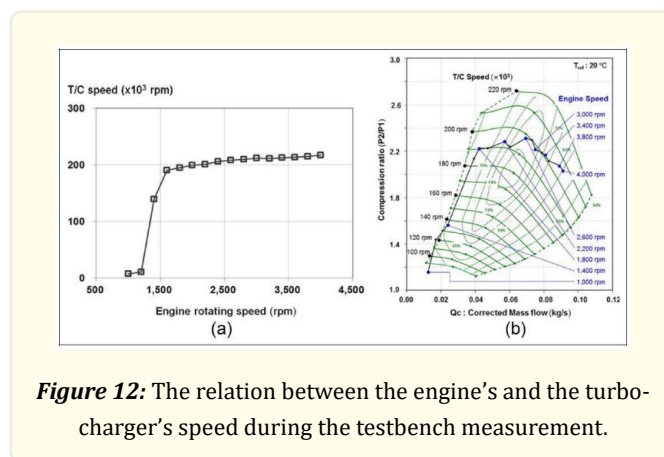


Figure 12: The relation between the engine's and the turbocharger's speed during the testbench measurement.

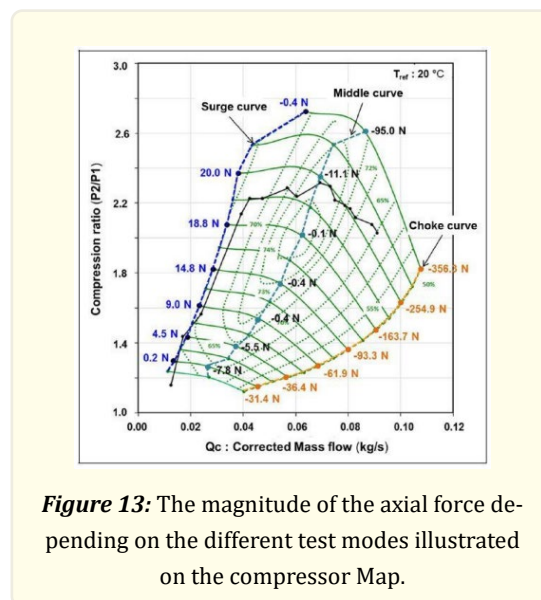
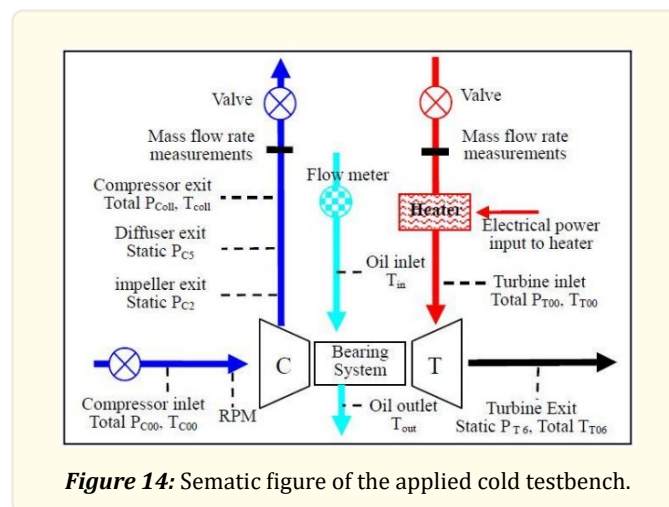


Figure 13: The magnitude of the axial force depending on the different test modes illustrated on the compressor Map.

The authors of [3] analyze turbocharger damage experienced during a flow-bench test, which was caused by the excessive axial load.

The tightening of the emission control regulations and the increase of the efficiency of the internal combustion engines, ensuring their proper power level, require an increasing pressure ratio on the turbocharger compressor side. In addition, it is also necessary to increase the turbine side expansion ratio to achieve better efficiency. The listed requirements appear as increasing axial forces in the turbochargers, the direction and magnitude of which varies with the speed of the charger [9]. Due to the narrow tolerance ranges and small joint clearances used for good efficiency, after a certain level of axial force, the charger can be seriously damaged.

To illustrate the dependence on axial force geometry, measurements were made with an original and a modified design. The newly installed compressor was capable of producing a higher pressure ratio. In the first case, the charger failed to perform the prescribed test program without damage, but the modified design produced damage and failure at a rated speed of 88%. In order to minimize temperature factors as much as possible, the measurements were carried out on a cold test bench, the outline of which is illustrated in the figure below.



The turbine is supplied with air by the compressor. The compressed air then heats up with the aid of an electric heater, but the temperature values are still far from the actual conditions, so it is still a cold test bench.

In two work points (at 52 and 80% rated turbo speed), measurements were made with the original and the modified geometry. Figure 15 shows these test results and a test measurement at a nominal speed of 88%. In the latter case, the turbocharger suffered damage after a short run.

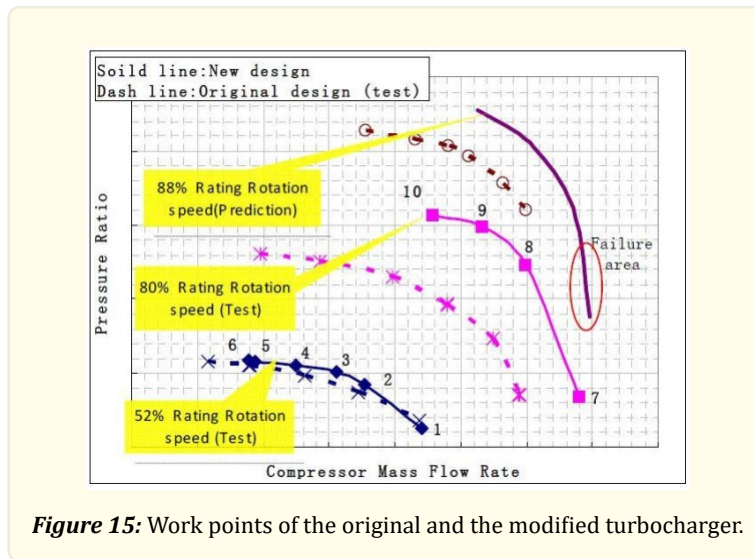


Figure 15: Work points of the original and the modified turbocharger.

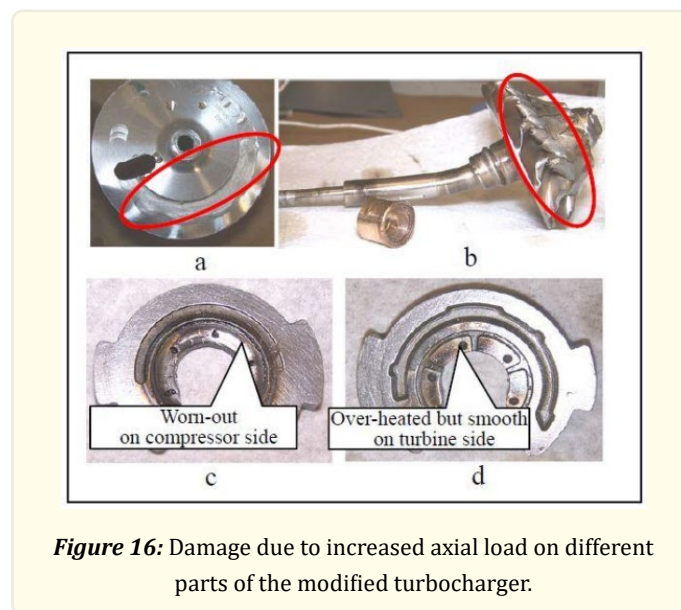


Figure 16: Damage due to increased axial load on different parts of the modified turbocharger.

It can be clearly seen that the loads resulting from the changed geometry have led to serious damage in almost every element of the rotor. Part a, of figure 16 shows the burnt surface on the backside of the compressor wheel, the deformation of the turbine blades on part b, the deflection of the shaft, and the excessive frictional force on the axial bearing on c and d.

At the two work points mentioned above (52 and 80% nominal speed), the following results were published with the help of a special simulation software at a nominal speed of 88%. The diagrams show the components of the axial forces on the compressor side and on the turbine side by, and the blue line shows the resultant.

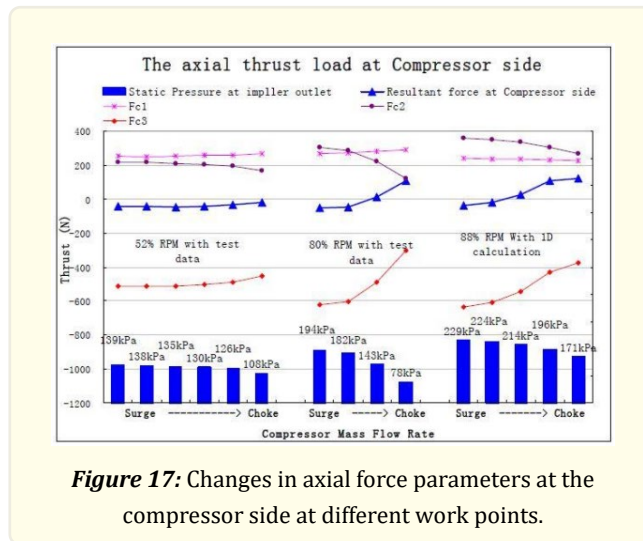


Figure 17: Changes in axial force parameters at the compressor side at different work points.

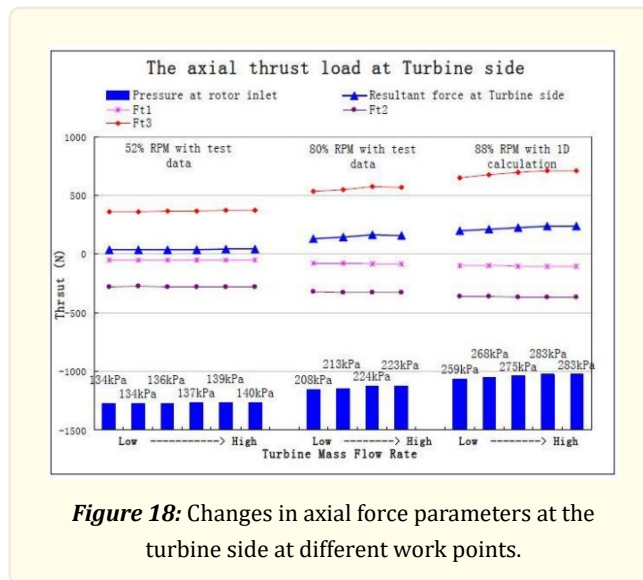


Figure 18: Changes in axial force parameters at the turbine side at different work points.

We can see that several measurements have been made at the given speeds, from the surge limit to the choke limit. Another figure shows the actual axial force resulting from the summing of the compressor and turbine side forces.

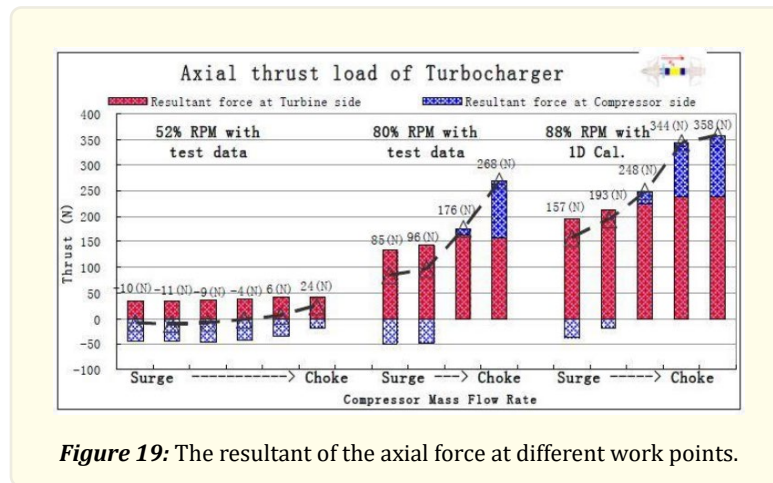


Figure 19: The resultant of the axial force at different work points.

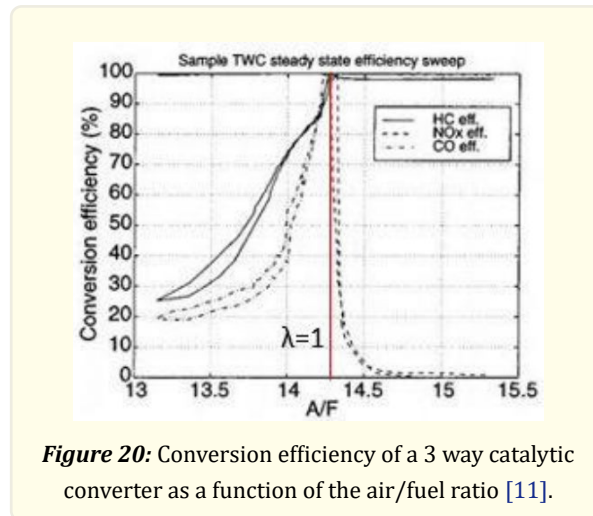
Under real conditions, the temperature of the gas entering the turbine is an important factor in calculating the axial force, and thus the effect of the change in load due to the increased expansion ratio. With the help of the previously mentioned 1D simulation program, it can be observed that the axial force decreases significantly with a temperature increase of 200 °C. This is due to the fact that, with the same turbine power, the increased inlet temperature requires a smaller expansion ratio, which is a lower inlet pressure, thus lower back pressure at the turbine wheel. Since the back pressure of the turbine wheel shows a positive force as well as the resulting axial force, the axial load decreases for the reasons mentioned above.

Analysis of the effect of newly introduced emission standards on axial force

In this part of the documentation, further testing options are listed to quantify the axial force of turbochargers, primarily dictated by the predicted environmental standards of the future, based on the results and methods of the literature presented in the previous chapters. The examinations are based on the Széchenyi István University's Department of Internal Combustion Engines, which has been specially developed for testing turbochargers, but in some cases, only theoretical implementation is announced. We want to create the measurements both in components and in combined installation and modelling the real conditions, concentrating on the lambda 1 operation and on the changing p4 pressure value caused by the different elements of the exhaust gas aftertreatment (e.g Otto particulate filter: OPF).

Lambda 1

In the case of Otto motors, the optimum operation of the three way catalytic converter, i.e. the neutralizing effect of the pollutants, is at the air/fuel ratio of 14,314,4 ($\lambda=1$) ie in the case of a stoichiometric mixture. In this state, there is almost exactly the same amount of nitrogen oxide (NOx) in the exhaust gas that can oxidizes the whole amount of the unburned hydrocarbons (HC) and carbon monoxide (CO) to carbon dioxide (CO₂) and water (H₂O). In this operating state, this neutralization is effective at over 90-95% [10]. The characteristic of these types of engines is that the knocking limits increase in performance and efficiency. In order to reduce the temperature during compression, the pre-ignition angle must be set closer to the top dead centre, thus avoiding this negative effect. However, the disadvantage of starting a combustion process closer to the top dead centre is that the efficiency of the engine is reduced and the heat load of the components of the exhaust system (exhaust valves, catalyst) and of the turbocharger (turbine housing, turbine shaft, bearings) can increase significantly. Another option is to reduce the charge pressure (which, however, means a reduction in performance), and to enrich the blend to avoid knocking. However, in the latter state ($\lambda < 1$), there is not enough nitrogen oxide to oxidize the increased amount of HC and CO, so the efficiency of the catalyst is reduced, resulting in an increase in HC and CO emissions [11] that could be no longer able to comply with the predicted environmental standards of the future. Therefore, it is necessary to operate the Otto motors with the lambda 1 at the widest possible range of operation.



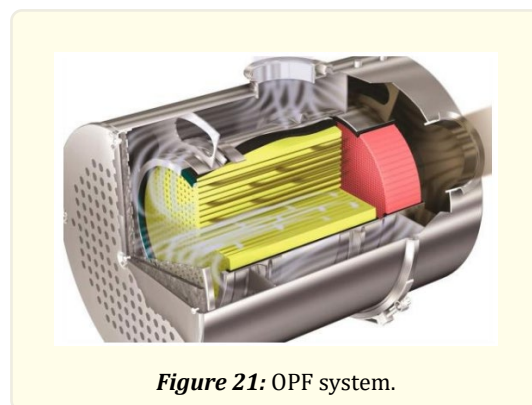
However, at a high load level, this means a significant increase in heat load, since there is no cooling effect due to the evaporation enthalpy of the previously burnt fuel. Thus, in our current investigations, we have to calculate a higher T3 value from the perspective of the turbocharger, which, according to the formulas presented earlier, affects the degree of axial force that is formed. With the help of the hot gas test bench, by measuring the above mentioned axial force-influencing parameters of the previously described literature, we can quantify this effect with the necessary calculations in addition to the mentioned T3 characteristic.

Measuring methods

The different physical heavens that have just been introduced are measured using sensors. After the necessary calibration and the software processing of the measured data is generated, this measurement process is primarily caused by the change of the already mentioned turbine-side inlet temperature (T3). Our aim is to map the effect of the temperature range up to 1000 °C on the axial force.

Backpressure growth (Otto Particulate Filter: OPF)

In the case of direct injection Otto motors, it is worth examining the impact of the incorporation of the particulate filter, which has become almost a basic requirement of environmental standards, into the axial force present in the turbocharger.



This component unit also generates backpressure like the catalysts and other elements in the exhaust system in the flow channel, which increases the value of the parameter after the turbocharger, i.e. the parameter p_4 , among the values listed in the documentation. The following methods are recommended for determining this effect and for examining its effect on axial force:

Engine testbench

The effect of the presence of the filter can be observed by replacing the gradient of the particulate filter caused by the engine testbench conditions during clogging by the change in the pressure value (p_4) measured after the turbine in the formulas previously described for determining the axial force in the turbocharger.

Hot gas testbench

Using the results of the engine test measurements, perform a specific cost and time efficient test specific to the given OPF on a testbench for turbochargers. Various control valves in the test bench can be used to set any p_4 value that allows us to perform very efficient testing.

Cold gas component testbench

The level of particle filter clogging and the resulting backpressure characteristic for a system with a given geometry can be recorded during engine testbench operation. In order to reduce costs, this characteristic allows further measurements to be made on a cold-test component test bench. Then, with a controlled, electrically actuated throttle valve (placed after the catalytic converter) can be used to generate the backpressure measured during the engine brake test. For more accurate measurement and reproducibility, it is advisable to place a pressure sensor both in front of the particulate filter (p_5) and thereafter (p_6) during the engine testbench measurements, and then apply this pressure ratio to the throttle before and after the throttle adjustment section.

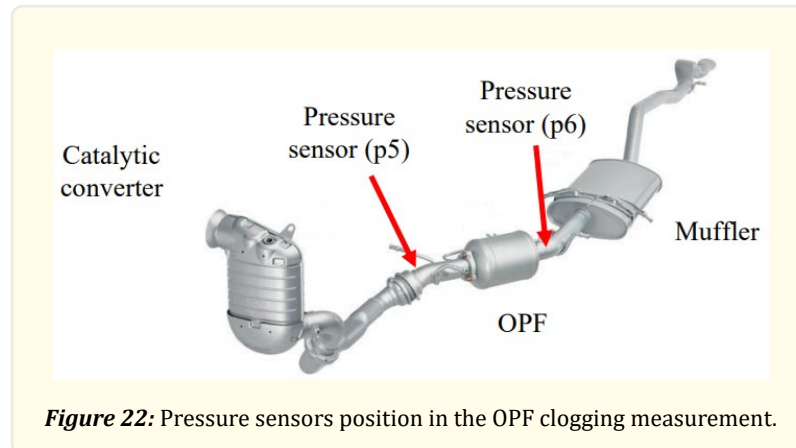


Figure 22: Pressure sensors position in the OPF clogging measurement.

Multi-stage turbocharging

In order to increase the charge level of internal combustion engines, it is necessary to produce a high pressure ratio on the compressor side, which requires an increased compressor wheel size. However, due to the deterioration of the dynamic properties of the turbocharger and the significant increase in rotor mass above a certain size, we cannot achieve the desired goals. In multi-stage charging, the multiple (typically two), connected to each other, can be used to increase the charge pressure without these negative effects. For this type of turbocharger, the charger units are practically transported to one another. Exhaust from the cylinders, driving the first turbine, continues to the second turbine, where another expansion occurs. From the compressor wheels so driven, the ambient air contact pre-compresses the air for the second compressor, thus further compressing the medium from a higher pressure level. With this system, the level of critical pressure increases as a whole, resulting in higher filling pressure.

Before to the second compression of the medium, the higher pressure level present on the inlet side of the compressor as a result of operation may can cause increased axial force from the compressor to the turbine based on the experience gained from the publications. The need for a continuously increasing pressure ratio can be as high as a significant additional burden in the above-mentioned relationship, so it is worth examining its effect.

VTG

To reduce the lag of the turbocharged engines, a flap unit for variable turbine inlet geometry was created, it is called VTG (variable turbine geometry).

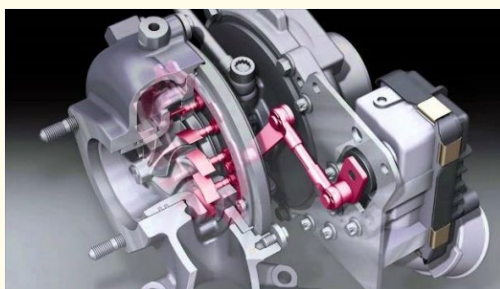


Figure 23: The mechanism of the VTG system.

A further advantage of the construction is the above-mentioned dynamic feature, that even in the case of monoturbo, a bigger compressor and turbine can be used as its acceleration properties do not deteriorate due to the VTG. In the following, we examine the effect of the presence and operation of this device on the axial force in the turbocharger. In this case, the measurement can only be performed on a turbocharger equipped with VTG.

Low and middle engine speed range

The exhaust flow channel has a higher back pressure due to its closed or slightly open position of the guide vanes, i.e. the value of p_3 increases.

High engine speed

In this case, the system operates as a quasi-normal turbocharger, so the axial force vector has the characteristics defined by turbine and compressor geometry.

Conclusion

The progressively tightening exhaust gas emission standards, as well as the current customer demands, are challenging for turbocharger developers. This documentation is intended to provide an idea of these development processes so that the structure can continue to operate without damage, with good efficiency and safety.

Acknowledgement

The paper was written with the support of the project titled "Internationalisation, initiatives to establish a new source of researchers and graduates and development of knowledge and technological transfer as instruments of intelligent specialisations at Széchenyi István University" (project number: EFOP-3.6.1-16-2016-00017).

References

1. Hung Nguyen-Schafer. "Rotordynamics of automotive turbochargers". 2. Edition, Ludwigsburg, Germany (2015): 150-155.
2. Kostandin Gjika and Gerald D Larue. "Axial load control on high speed turbochargers". Proceedings of ASME Turbo Expo 2008: Power for Land, Sea and Air GT2008 (2008).
3. In-Beom Lee, Seong-Ki Hong and Bok-Lok Choi. "Investigation of the axial thrust load using numerical and experimental techniques during turbocharger operation". Journal of automobile engineering (2017).
4. Wilcock DF and Booser ER. "Bearing design and application". McGraw-Hill, New York (1957).
5. Pinkus O and Sternlicht B. "Theory of hydrodynamic lubrication". McGraw-Hill, New York (1961).
6. Lamquin T and Gjika K. "Power losses identification on turbocharger hydrodynamic bearing system: test and prediction". ASME Turbo Expo 2009: power for land, sea, and air GT2009-59599 (2009): 153-162.
7. Hong H and Ma C. "Numerical solution of axial thrust of turbochargers". Veh Power Technol (2006).
8. Jizhong Zhang, et al. "Fault diagnosis and failure prediction by thrust load analysis for a turbocharger thrust bearing". Proceedings of ASME Turbo Expo 2010: Power for Land, Sea and Air GT2010 Glasgow, UK (2010).
9. Nicholas C Baines. "Fundamentals of turbocharging". Concepts NREC Inc, Vermont (2005).
10. Defoort M, Olsen D and Willson B. "The effect of air-fuel ratio control strategies on nitrogen compound formation in three-way catalysts". International Journal of Engine Research 5.1 (2004): 115-122.
11. Brandt EP and Yanying Wang and Grizzle JW. "Dynamic modeling of a three-way catalyst for SI engine exhaust emission control". IEEE Transactions on Control Systems Technology 8.5 (2000): 767-776.

Volume 4 Issue 4 April 2023

© All rights are reserved by Richárd Takács.